Article

Hydrodynamic Cavitation of Creosote Oil in the Presence of a Ni^{2+} Initiator Results in an Increase in Its Overall Naphthalene Content

Yu-Fang Ye,* Ying Zhu, Zhi Su, Feng-Yun Ma, and Ting Liang

ACCESS | Metrics & More | Article Recommendations

ABSTRACT: Hydrodynamic cavitation (HC) of aromatic hydrocarbons present in creosote oil obtained from coal tar in the presence of 0.3% (w/w) Ni^{2+} as an inducer increased its naphthalene and phenanthrene content by 7.3 and 2.6%, respectively. An optimal procedure was developed based on the use of an upstream pressure of 2.6 MPa, an immersing height (H) for the cavitator of 105 mm, 10% H$_2$O content, use of a NiSO$_4$ solution at pH 4.0, and an operating temperature of 75 °C. Enrichment of the naphthalene and phenanthrene components is caused by hydroxyl and hydrogen radicals generated in the reaction inducing aromatic components to undergo a series of radical demethylation/methylation reactions to produce new product ratios. The observed increases in naphthalene and phenanthrene content using Ni^{2+} as a radical inducer are in contrast with the previous results using Fe^{2+} under similar conditions, which led to the enrichment of the acenaphthalene fraction of creosote oil.
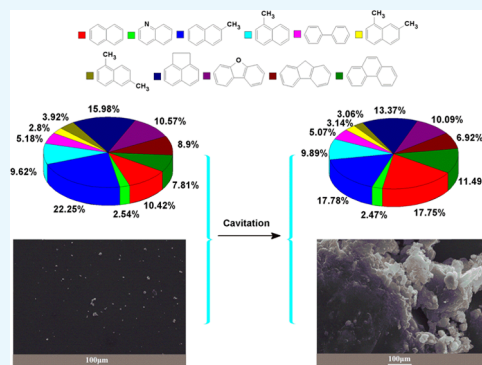
1. INTRODUCTION

More than 500 different types of organic compounds have been identified in coal tar, with many of its components being extremely useful as raw materials for the production of plastics, synthetic rubbers, synthetic fibers, dyes, pesticides, and medicines.[1] Furthermore, some of the polycyclic and hetero-cyclic compounds that it contains are difficult to obtain from other sources or cannot be prepared economically using synthetic routes. Therefore, coal tar represents a precious natural organic hydrocarbon source from which existing/new chemicals can be isolated. The creosote oil fraction accounts for around 9% of coal tar, which is a mixture of volatile components that boil over a range from 218 to 340 °C that are mainly comprised of bicyclic and tricyclic aromatic hydrocarbons.[2] Creosote oil is a complex mixture containing over 50 types of aromatic hydrocarbons, including naphthalene, quinoline, methyl naphthalene, biphenyl, dimethyl naphthalene, acenaph-thene, dibenzofuran, fluorene, and anthracene (phenanthrene).[3] However, the abundance of individual components in creosote oil is generally low, with 2-methyl-naphthalene having the highest content at 20%, and only 11 other compounds exceeding 1%. Therefore, it is difficult to economically separate creosote oil into its pure constituents using the commonly available industrial separation technologies.

Hydrodynamic cavitation (HC) refers to the process of formation, growth, and collapse of cavities (cavitation) caused by the change in the liquid pressure field during a liquid flow.[4] A large number of small holes in the liquid generated shock waves and microjets in the process of collapse, resulting in a strong collision and mixing between liquid particles so that different

components of the liquid can be fully mixed, especially in the liquid—liquid heterogeneous system, which can achieve the emulsion state. Thanekar et al.[5] studied the combination of HC and oxidant in the treatment of industrial wastewater. The optimal pretreatment method of HC + O$_3$ can reduce the chemical oxygen demand (COD) by 40%, and the further activation of the sewage treated by the HC + O$_3$ process can reduce COD by about 89.5% after sludge treatment. The biodegradation index increased from 0.35 to 0.75 by the HC + O$_3$ pretreatment. Yi et al.[6] studied the decomposition of Rhodamine B (RHB) by hydrodynamic method (HC) and acoustic method (AC) and the combination of the two methods. Both hydrodynamic and acoustic degradation can be carried out in the same space. The effects of initial concentration, inlet pressure, solution temperature, and ultrasonic power were studied and discussed. A clear synergy has been found in this process. Under the condition of ultrasonic power of 220 W and treatment time of 30 min, the highest conversion rate of the hydraulic ultrasonic cavitation system can reach 119%, which greatly increases the degradation efficiency of the hydraulic cavitation. Cai et al.[7] explored the dewatering of waste-activated sludge by integrated hydrodynamic cavitation (HC) and Fenton

reaction and revealed the synergism of the HC/Fenton treatment. The results indicate a three-step mechanism, namely, the HC fracture of different extracellular polymeric substances (EPSs) in sludge flocs, Fenton oxidation of the released EPS, and Fe(III) reflocculation, which is responsible for the synergistically enhanced sludge dewatering. Boczkaj et al.[8] studied the combination of HC and other oxidation processes (O_3/H_2O_2/Peroxone) for the treatment of asphalt production wastewater (initial COD was in the range of 8000−12 000 mg/L). The results showed that the maximum reduction rates of COD and biological oxygen demand (BOD) were 40 and 60%, respectively.

The goal of this research project was to present a systematic study of the HC process focusing on the increase in the naphthalene content of creosote oil to improve its overall value in an efficient and economical manner.

2. EXPERIMENTAL SECTION

2.1. Properties of the Creosote Oil Sample. The creosote oil sample from coal tar was a mixture of fractions collected over a range of boiling points from 218 to 340 °C, whose major components were bicyclic or tricyclic aromatic hydrocarbons. The creosote oil was supplied by Xinlian coal chemical company, Xinjiang, China. Table 1 lists the boiling points and the relative ratios of the components in the oil sample, which had an initial naphthalene content of 10.42%.

Table 1. Properties and Relative Content of the Components in the Oil Sample

no.	components	retention time (min)	boiling point (°C)	relative content (%)
1	naphthalene	19.004	218	10.42
2	quinoline	19.967	237	2.54
3	2-methyl-naphthalene	21.047	241	22.25
4	1-methyl-naphthalene	21.365	246	9.62
5	biphenyl	22.411	256	5.18
6	1,7-dimethyl-naphthalene	22.894	263	2.80
7	1,6-dimethyl-naphthalene	23.148	265−266	3.92
8	acenaphthene	24.337	278	15.98
9	dibenzofuran	24.814	287	10.57
10	fluorene	25.861	293	8.90
11	phenanthrene	28.875	340	7.81

2.2. Experimental Setup. The HC setup used in these experiments is shown schematically in Figure 1, which comprised of a cavitator, gear pump, pipe, and vertical tank with a height of 500 mm and a diameter (D) of 132 mm. The cavitator was tubular with a length (L) of 150 mm and a diameter (d_1) of 30 mm, which was fitted with a venture tube that contained a throat with a diameter (d_2) of 18 mm. It contained two orifice plates that were 5 mm thick, with diameters of 30 mm, which contained eight holes of 2 mm diameter (d_3). The cavitator was fitted with an upstream pressure gauge and a turbine flowmeter to monitor the stability and flow rates of the reaction. A bimetallic thermometer in the tank functioned to determine the reaction temperature, which was cooled to −15 °C to reduce the rate of reaction and prolong the reaction time (Figure 2).
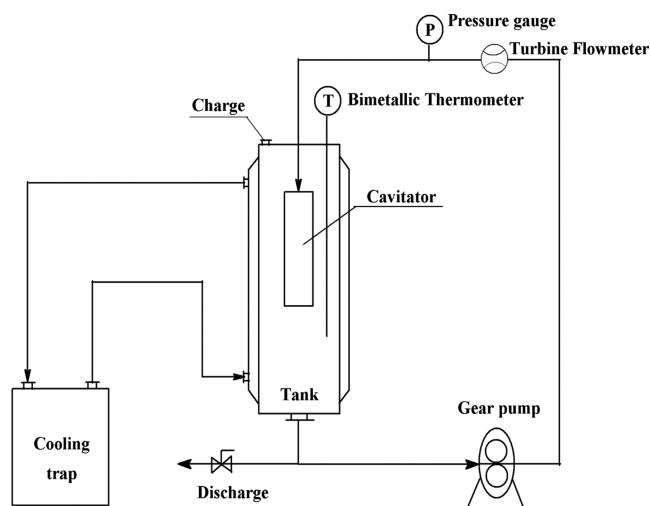

Figure 1. Schematic representation of the hydrodynamic cavitation reactor setup.

2.3. Choice of Inducing Agent. Previous work has shown that inducers can have a significant influence on the outcome of the HC treatments of creosote oil.[9] For example, Fe^{2+} ions have been used as an inducer to produce H• radicals that react with naphthalene, 1-methyl-naphthalene, 1,7-dimethyl-naphthalene, dibenzofuran, and phenanthrene to selectively produce acenaphthene. In this work, Ni^{2+}, Co^{2+}, $(Mo_7O_{24})^{6-}$, and 1:1 mixtures of Ni^{2+}/Mo^{6+} salts were screened as potential inducers.

2.4. Analysis and Preparation of Feedstock. A Karl−Fischer moisture meter was used to determine the water content of the samples. $NiSO_4 \cdot 6H_2O$ (0.8% (V/V)), $CoSO_4 \cdot 6H_2O$, $(NH_4)_6Mo_7O_{24} \cdot 4H_2O$, or $FeSO_4 \cdot 7H_2O$ were weighed in accordance with the amount of Ni^{2+}, Co^{2+}, $(Mo_7O_{24})^{6-}$, or Fe^{2+} required, respectively. The $NiSO_4$ solutions were prepared by dissolving $NiSO_4$ in water, and H_2SO_4 (1 M) was used to adjust the pH of solutions to the desired value before they were mixed with oil samples.

2.5. Experimental Process and Sample Analysis. Experiments were carried out using natural cooling, external cooling from the start of the reaction, or external cooling to keep the reaction temperature below 30 °C, respectively. Figure 3 shows the conversion rates for the three different temperature conditions over time, with external cooling resulting in longer reaction times (see Table 2). The circulation of the feedstock was driven by a gear pump until the reaction was complete, with the feedstock then transferred to a tank and cooled to 0 °C through the action of a cooling trap under an upstream pressure at 2.6 MPa with an immersion height of the cavitator being 105 mm. A control experiment revealed that no change in the composition of the oil samples occurred in the absence of ultrasonic agitation.

Oil samples were withdrawn from the reaction mixture and cooled to ambient temperature before their composition was determined by gas chromatography (GC) (GC-MS 2010, Shimadzu Corporation, Japan) analysis. The GC conditions using the following conditions: injection port at 280 °C and detector at 250 °C, the initial temperature of 50 °C for 1 min, followed by an increase to a maximum temperature of 280 °C at the rate of 8 °C/min. The elastic quartz capillary column was HB-5 with a neutral phase (60 m × 0.25 mm × 0.25 μm); other experimental details were identical to those reported previously.[9]
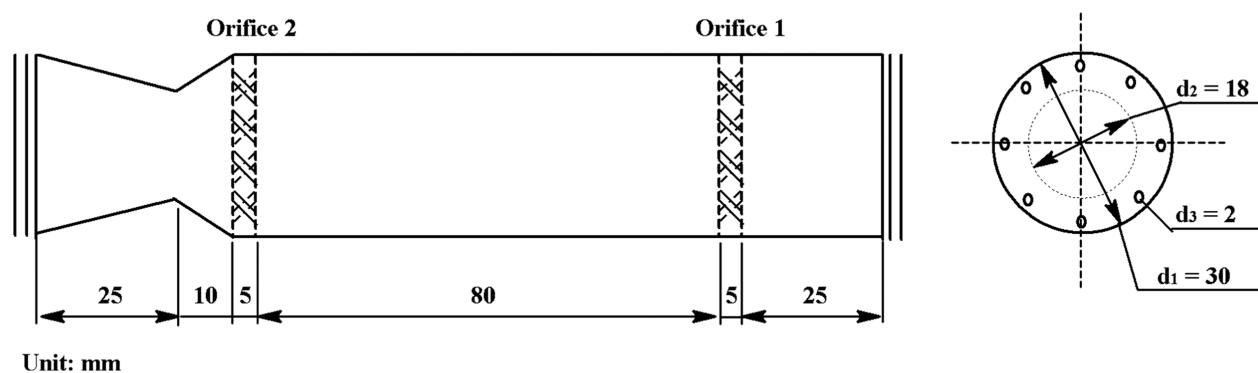
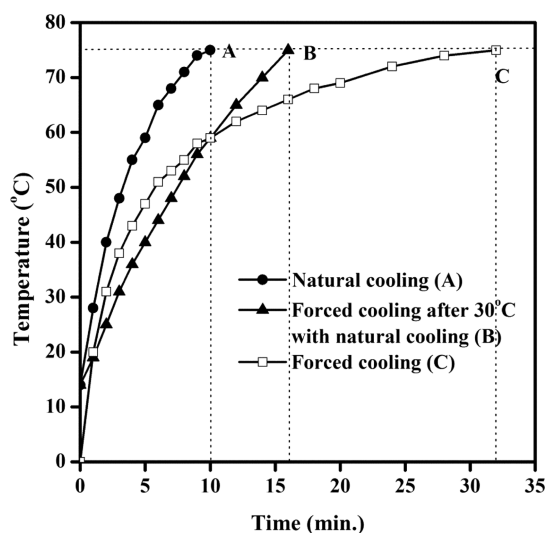**Figure 2.** Schematic representation of the cavitating device.

Figure 3. Temperature curve with the time of cavitation under different types of cooling.

Table 2. Temperature Rates by Piecewise Regression

curve	time (min)	function	R^2	function
(A)	≤3	$T = 13t + 14$	0.99	heating
	3−10	$T = 4.3t + 37$	0.99	reacting
(B)	≤3	$T = 5.5t + 14$	0.99	heating
	3−10	$T = 4.1t + 19$	0.99	reacting
	10−16	$T = 2.65t + 33$	0.99	
(C)	≤3	$T = 15t + 2$	0.94	heating
	3−10	$T = 3.2t + 30$	0.97	reacting
	10−32	$T = 0.7t + 54$	0.98	

3. RESULTS AND DISCUSSION

3.1. Hydraulic Features. The ratio (β) of the total flow area through the holes of the orifice (A_N) to the upstream pipe surface (A_P) can be written as follows

$$\beta = A_N/A_P$$

$$\because A_N = 8 \times \pi d_3^2/4, \quad A_P = \pi d_1^2/4$$

$$\therefore \beta = (d_3/d_1)^2 \times 8 = (2/30)^2 \times 8 = 0.036 \quad (1)$$

According to the distributions along fraction for water at 25 °C in the hydrodynamically cavitation flow field have been simulated with the help with the directions of axial and radial of pressure, velocity and vapor volume of κ-ε model in the computational fluid dynamic (CFD) (see Figure 2). The results

of these modeling studies for section S_{1-1} are shown in Figure 4a−c, with cylindrical coordinates established with reference to the center of the cavitator, and the quotient r/r_0 defined as a normalized radius.

Figure 4a shows that the pressure distribution reduced from 2.6 to 0 MPa along the axial direction, with the pressure reducing from 2.6 to 1.7MPa as the suspension flowed through the first orifice and from 1.7 to 0 MPa as the suspension flowed through the second orifice. After section S_{1-1} the pressure was 0.04 MPa for an r/r_0 of 0 to 0.6, increasing to 0.76 MPa for a r/r_0 of 0.6−1 in a radial direction. Figure 4b reveals that the water velocity reached the maximum value of 50.94 m/s within the holes of orifice 2. The velocity increases from 0.031 to 17.0 m/s flowing through the first orifice to 40.3 m/s near the wall through the second orifice in an axial direction. After the second orifice, the velocity increases in turn with the radial direction from 0.031 to 12.76 m/s for r/r_0 = 0 to 0.4; from 19.12 to 33.97 m/s for r/r_0 = 0.4 to 0.6, and from 36.08 to 40.33 m/s for r/r_0 = 0.6 to 1. Figure 4c shows that the S_{1-1} vaporization section reaches a maximum value of 98.7% at r/r_0 = 0 and then reduces from 98.7 to 0% for r/r_0 equal to 1. Hydraulic characteristics of the cavitator were calculated from the cavitation number (C_v), which is a dimensionless number that describes the cavitation efficiency in hydraulic devices.[10−12] This number is obtained using the following equation

$$C_v = \left(\frac{p_2 - p_v}{(1/2)\rho v_0^2} \right) \quad (2)$$

where p_2 is the fully recovered downstream pressure, p_v is the saturated vapor pressure of the water at 0.0385 MPa, v_0 is the water velocity as it exits orifice 2, and ρ is the water density of 924 kg/m³.

Figure 5 shows the effect of r/r_0 and the cavitation number (C_v) on the downstream pressure (Figure 5a), water velocity (Figure 5b), and water vapor volume (Figure 5c) values at orifice 2, respectively. These results reveal that larger r/r_0 values lead to increased pressures and water velocities while the water vapor volume fraction decreased with an increase in r/r_0. Changes in the cavitation number follow an upward parabolic curve with increasing r/r_0, with a minimum value of 0.2 at r/r_0 = 0.7 visible in Figure 5a−c. Cavities were only produced in large numbers when $C_v \leq 1$; therefore, effective cavitation is only produced for r/r_0 values ranging from 0.24 to 1 in this device.

3.2. Effect of H₂O Content on Product Distribution. The effect of water on the amount of naphthalene content produced in the cavitation process was explored by conducting experiments with 5, 7, 10, and 15% water content (see Figure 6),
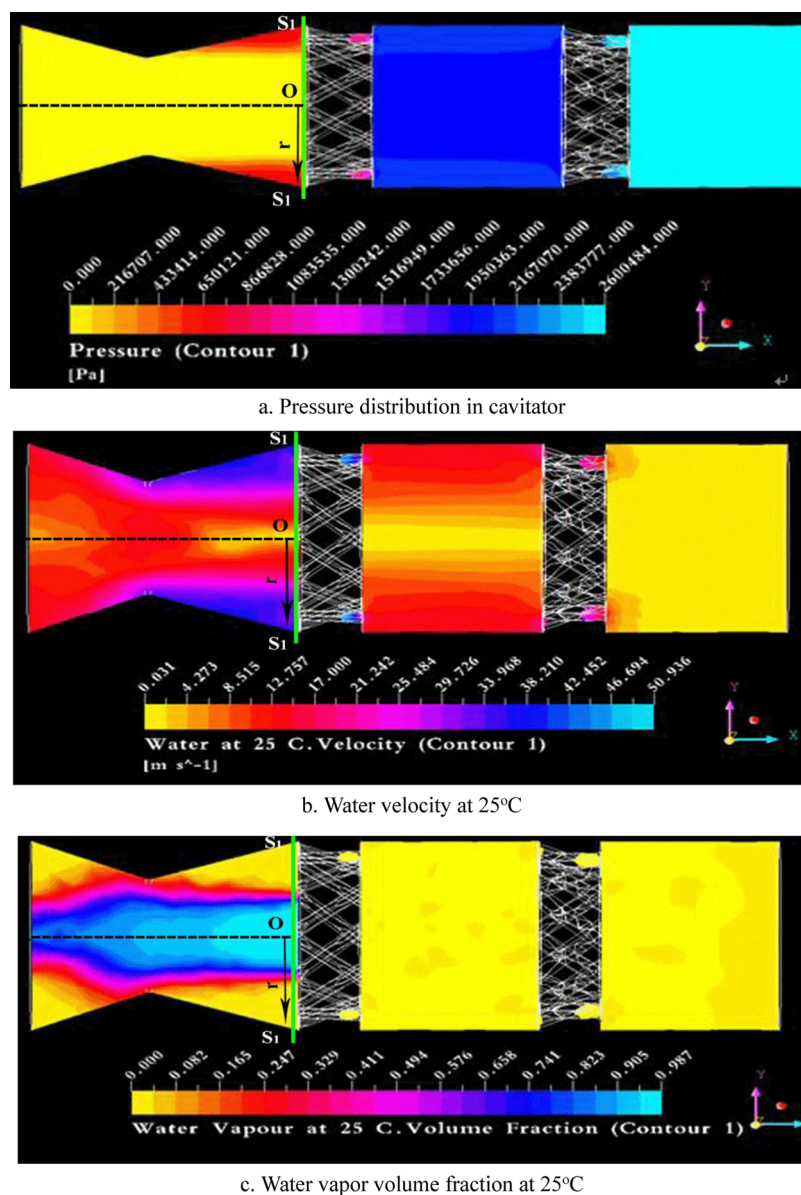
a. Pressure distribution in cavitator

b. Water velocity at 25°C

c. Water vapor volume fraction at 25°C

Figure 4. CFD simulation diagrams of cavitator. (a) Pressure distribution in cavitator, (b) water velocity at 25 °C, and (c) water vapor volume fraction at 25 °C.
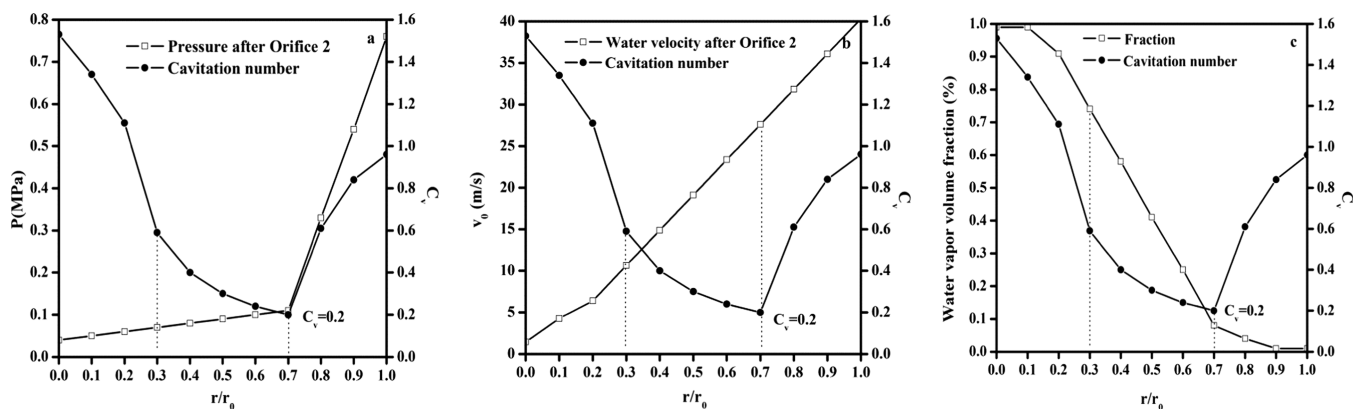

Figure 5. Relationship among r/r_0 of cavitator, cavitation number (C_v) and downstream pressure (a), water velocity (b), and water vapor volume (c) after orifice 2, respectively.

which revealed a maximum 5.77% increase in naphthalene for the water content of 10%. The ultrasonic cavitation of water in the system results in its homolytic cleavage to afford hydrogen and hydroxyl radicals (e.g., $H_2O \rightarrow H^\bullet + HO^\bullet$),[13] with the

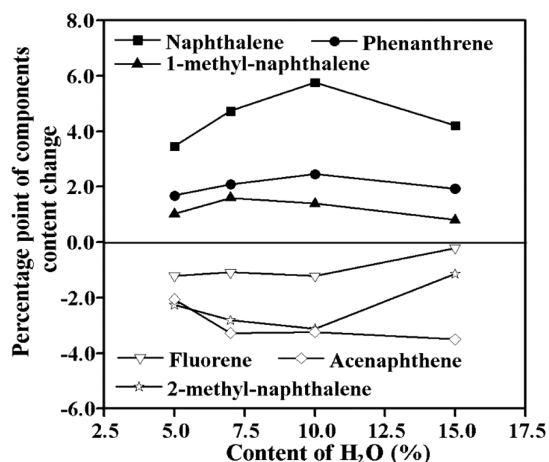**Figure 6.** Effect of the initiator H_2O amount on the component content change of product.

Figure 7. Effect of reaction time on the component content change of product.

biphasic reaction being efficiently mixed to form an emulsified colloidal system as it flows through the cavitator. The relatively high boiling range of 218−340 °C of the aromatics (see Table 1) in the cavitator means that a highly emulsified and dispersed colloidal water/oil (W/O) and vapor/liquid (V/L) systems are generated. The vaporization rate of water in the cavitator exceeds 98% at 25 °C, meaning that all of the water in the material is essentially vaporized, which results in an increase in pressure when the oil feedstock meets the swirling interface that results in all of the vapor bubbles rapidly collapsing under such high pressure.[14]

This results in very strong shock waves and microjets being produced, which provide sufficient energy to the system for the aromatic components to be equilibrated to produce a greater proportion of lower-energy aromatics.[15] The sonication process produces shock waves reaching 140−170 MPa with a frequency of 100−1000 Hz, which results in the homolytic dissociation of H_2O and O_2, which produces highly active $H^\bullet$, $HO^\bullet$, and $O^\bullet$ radicals, respectively. The impact energy depends on the literature.[16] There is almost no heat transmission resistance or mass transfer resistance when the bubbles collapse;[17] however, bubble collapse promoted a more intense contact between the oil components and $H^\bullet$, $HO^\bullet$, and $O^\bullet$ radicals to promote the overall reactivity of the system.[18,19]

3.3. Effect of the Reaction Time on Naphthalene Yield. Monitoring the cavitation reaction of creosote under constant conditions over time (10−90 min) revealed that the maximum yield of naphthalene obtained was 5.77%, when the reaction time crossed 32 min, with its yield then declining slowly over the next 60 min. The maximally increased phenanthrene was 2.60 after 60 min, with its yield then declining slowly over the next 30 min (see Figure 7). Because the reaction to produce phenanthrene needs more energy than that to produce naphthalene. Therefore, there is a need for a longer reaction time.

3.4. Effect of the Inducing Agents. The effect of using different inducing agents (at a 0.3% level) in the ultrasonic reactions of creosote oil was investigated using 10% H_2O, 10% at an operating temperature of 75 °C (see Figure 8).

Similar product profiles over time were observed for Co^{2+}, $[Mo_7O_{24}]^{6-}$, and Ni/Mo = 1:1 and Ni^{2+} catalysts (e.g., increased naphthalene and phenanthrene content), which were different from those obtained by the use of Fe^{2+} catalysts (e.g., increased acenaphthalene content). When Ni^{2+}, Co^{2+}, $[Mo_7O_{24}]^{6-}$, and
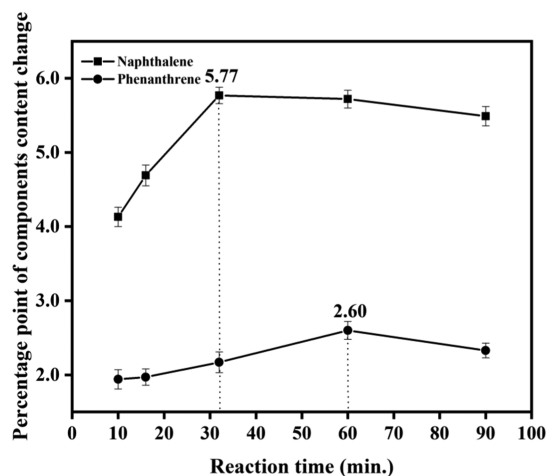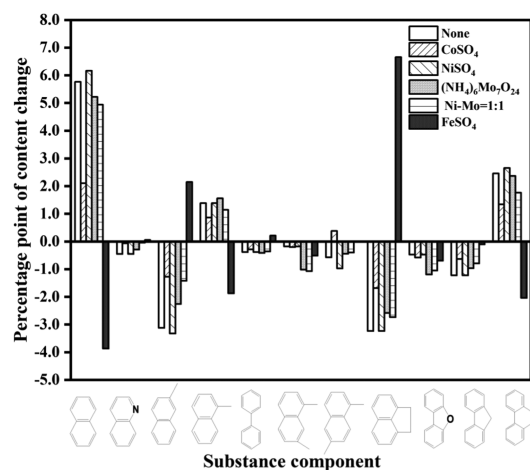

Figure 8. Effect of different inducing agents on the component content change of product.

Ni/Mo = 1:1 were used as inducers, the contents of naphthalene, 1-methyl-naphthalene, and phenanthrene in creosote were found to increase, whereas the amounts of 2-methyl-naphthalene, acenaphthene, dibenzofuran, and fluorene were decreased. The greatest increase in the naphthalene content of 6.17 percentage points was achieved when Ni^{2+} was used as an inducer, with the naphthalene yield using $Ni^{2+} > [Mo_7O_{24}]^{6-} > $ Ni/Mo = 1:1 $> Co^{2+}$. The result of Fe^{2+} as the inducer has been published by our team in the previous work.[11] The reason for this result might be that Ni^{2+}, Co^{2+}, $[Mo_7O_{24}]^{6-}$, and Ni/Mo = 1:1 were inducers of common hydrogenation. However, Fe^{2+} might react with $HO^\bullet$ under these conditions, which was the Fenton reaction; therefore, more strong oxidizing free radicals were released. In ref 8, the acenaphthalene content of Fe^{2+} is increased at 75 °C. However, the naphthalene yield of Fe^{2+} is relatively increased at 90 °C and that of acenaphthalene decreased. The results of the two experiments were that the methyl metathesis reactions of the aromatic components occurred under thermodynamic control, except that the rate of the Ni^{2+} reaction was faster than that of the Fe^{2+} reaction. Therefore, although neither reaction fully reached an equilibrium, the Ni^{2+} reaction with more naphthalene and phenanthrene (stable) is closer to equilibrium than the Fe^{2+} reaction that contains more acenaphthalene (less stable).

Neither reaction reached a full equilibrium, which is why the naphthalene intermediate reacts further for extended reaction times.

3.5. Effect of Ni²⁺ Dosage. The effect of varying amounts of Ni^{2+} as an inducer was investigated over a range from 0 to 0.6 (wt %) using 10% H_2O at 75 °C, with an optimal loading of Ni^{2+} of 0.3% (see Figure 9). When Ni^{2+} was higher than 0.3%, the
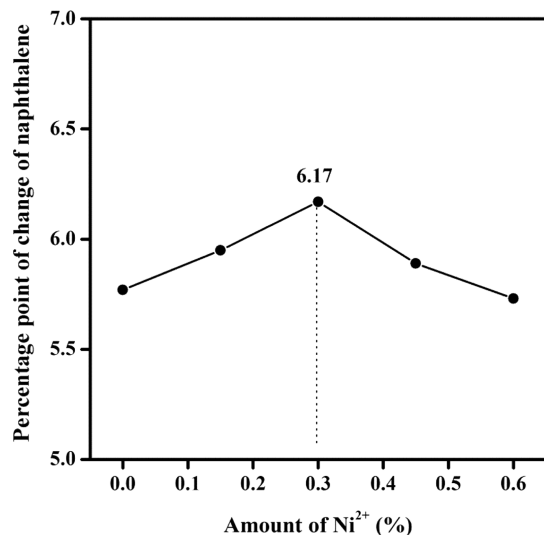

Figure 9. Effect of the amount of inducer of Ni^{2+} on the change in naphthalene.

surface tension increased. The largest surface tension caused the number of cavitation bubbles produced by cavitation to decrease, but the size of the grown bubble was increased and the energy released by the bubble collapse was enhanced.

3.6. Effect of pH of NiSO₄ Solution. pH effects were explored over a range from 1.0 to 6.0 using H_2SO_4 (1 M) to adjust the pH levels, with a maximum increase in naphthalene content observed at pH 4.0, which is consistent with the hydroxyl radicals being produced by ultrasonication under acidic conditions (see Figure 10). For example, Patil and Gogate[20] have reported that the HC degradation of aqueous
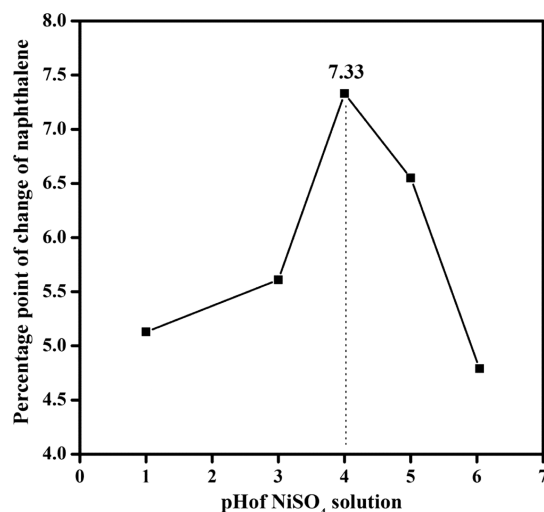

Figure 10. Content change of naphthalene with different pH of NiSO₄ solution of the product.

solutions of methyl parathion was greatest at a pH value of 3, while Shriwas and Gogate[21] reported that its ultrasonic degradation rate was fastest at pH 2.5. A decrease in pH will promote ultrasonication-mediated homolytic dissociation of water into HO• and H• during the cavitation process, while an acidic environment will promote the formation of more stable oil−water emulsions that will enhance the mass transfer effects and increase the reaction rates. The stability of the emulsions isolated from these cavitation reactions increased significantly at lower pH, with emulsions observed to be stable for more than 30 days at pH ≤4 (see Figure 11).
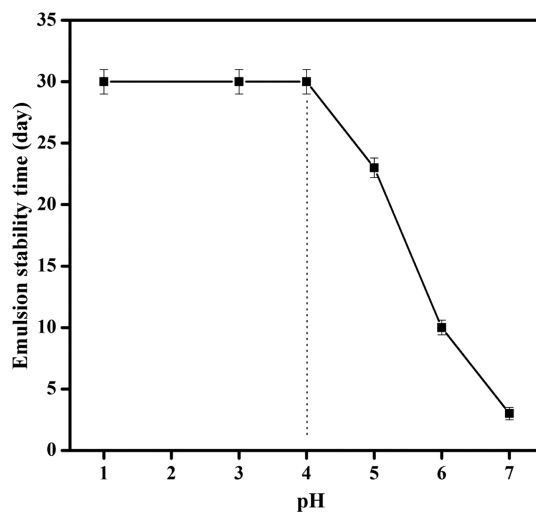
Figure 11. Emulsion stability time with different pH after cavitation.

3.7. Effect of Operating Temperature. The effect of temperature on naphthalene content was studied at different temperatures (60, 65, 70, 75, 80, and 95 °C) using 0.3% Ni^{2+} as inducer and H_2O 10% at pH 4.0, which revealed that maximal naphthalene (7.33%) and phenanthrene (2.6%) content was produced between 75 and 80 °C (see Figure 12). HC processes used for chemical modification normally have an optimal reaction temperature,[22] with gas solubilities generally decreasing as the temperature increases, which can result in reduced cavitation in the vaporization core of the ultrasonic process.

Figure 12. Effect of operating temperature on the component content change of the product.

Table 3. Material Balance Values of the Radical Reactions, Measured Values, and Comparison of Both

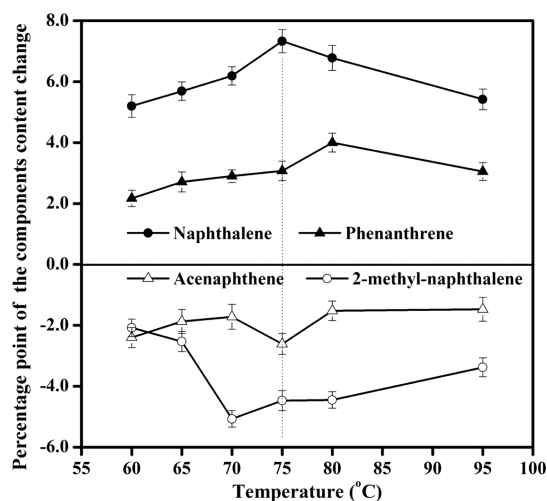| no. of reaction	reactants	reduce percentage points (w)	products	P/R molecular weight ratio	balance value	∑ balance value	increase percentage points (w)	relative error (%)
(2)	2-methyl-naphthalene	4.47	naphthalene	0.901	4.03	7.14	7.33	2.59
	1,6-dimethyl-naphthalene	1.04		0.900	0.94			
	acenaphthene	2.61		0.831	2.17			
(3)	dibenzofuran	0.48	phenanthrene	1.060	0.51	2.63	2.64	0.38
(4)	fluorene	1.98		1.072	2.12			

Figure 13. Reaction mechanism of creosote oil by hydrodynamic cavitation.

Furthermore, an increase in the vapor pressure of liquid enhances evaporation but can weaken cavity collapse, with reductions in liquid viscosity leading to a decline in the disturbance and the rate of cavity collapse.[23]

3.8. Reaction Mechanism and Products Formed in the HC Reaction. Optimal conditions for the ultrasonication of the creosote oil were established based on the use of an upstream pressure at 2.6 MPa, an immersion height at 105 mm, use of 0.3% Ni^{2+} as an inducer, 10% H_2O at pH 4.0, and an operating temperature of 75 °C. This reaction resulted in an increase in the amount of naphthalene present by 7.14% and an increase in phenanthrene content by 2.63% (see Table 3), which is consistent with the series of radical chain reactions shown in Figure 13.

3.9. Evidence for the Production of HO• Radicals in the Hydrodynamic Sonication Reactions. The cavitation conditions induce homolytic cleavage of water to produce highly reactive H• and HO• radical reactions that are responsible for reforming the aromatic substrates in the colloidal oil−water mixture (see Figure 13).[24] To verify the proposed mechanism, a solution of methyl violet (MV) (0.02 mmol/L) was sonicated in the cavitator system at rt for 13 min, which resulted in a final solution temperature of 60 °C. The absorption peak at a wavelength of 583 nm was found to decrease from 0.892 at the start of the reaction to 0.354 after cavitation, consistent with the HO• radicals reacting with methyl viologen to produce products with lower absorption values[25] (see Figure 14).
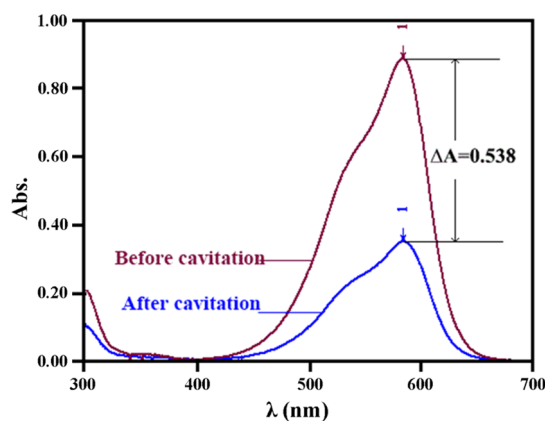

Figure 14. UV of methyl violet solution before and after the cavitation.

3.10. Calculations of Bond Dissociation Energies of Water and Aromatic Compounds. Based on the reaction mechanism proposed in Figure 13, the bond dissociation energies of HO−H, C_6H_5−OH, C_6H_5−H, $C_{10}H_7$−H, C_6H_5−CH_3, and $C_{10}H_7$−CH_3 were computed using a B3LYP/6 density

functional level, the results of which are shown in Table 4. The energy of the dissociation of H_2O into H• and HO• was calculated as 497.1 kJ/mol, which was in good agreement with the previously reported value of 499.0 kJ/mol.[26] The bond dissociation energies calculated for C_6H_5−OH was 487.5 kJ/mol, while $C_{10}H_7$−H and C_6H_5−H were both 473.3 kJ/mol and $C_{10}H_7$−CH_3 and C_6H_5−CH_3 were both 449.0 kJ/mol, respectively. These bond dissociation energy values were all less than the corresponding bond dissociation energies of H_2O, so it is clear that cavitation provides enough energy for homolytic cleavage of the O−H and C−H bonds of these aromatic compounds to occur.

4. CONCLUSIONS

Hydrodynamic cavitation (HC) of aromatic hydrocarbons present in creosote oil obtained from coal tar in the presence of 0.3% (w/w) Ni^{2+} as inducer increases its naphthalene and phenanthrene content by 7.7 and 2.6%, respectively. The following conclusions can be drawn to explain the increase in naphthalene content:

- Cavitation processes result in H_2O being homolytically cleaved into HO• and H• radicals that combine with Ni^{2+} species to facilitate demethylation of methyl-naphthyl naphthalene species by hydrogen radicals to afford naphthalene.

- A 7.33% increase in the naphthalene content (70% increase overall) of creosote oil has been achieved through its ultrasonication in the presence of 0.3% $NiSO_4$ and 10% H_2O (pH 4.0) at 75 °C.

- Evidence that the ultrasonication-mediated homolytic cleavage of water to generate hydrogen and hydroxy radicals was achieved using methyl viologen as a control substrate that was shown to rapidly decompose under the cavitation conditions.

Table 4. Bonds Dissociation Energies for Six Molecule Models

№	Reactant	Energy of reactant (Ha)	Product 1	Energy of product 1 (Ha)	Product 2	Energy of product 2 (Ha)	bond dissociation energy (kJ/mol)
1	H_2O	-76.37	HO·	-75.68	H·	-0.496	497.1
2	(phenol, OH)	-307.2	(phenyl radical)	-231.3	OH·	-75.67	487.5
3	(naphthalene)	-385.48	(naphthyl radical)	-384.8	H·	-0.496	473.3
4	(benzene)	-232.0	(phenyl radical)	-231.3	H·	-0.496	473.3
5	(methylnaphthalene, CH_3)	-424.8	(naphthyl radical)	-384.8	·CH_3	-39.78	449.0
6	(toluene, CH_3)	-271.3	(phenyl radical)	-231.3	·CH_3	-39.78	449.0

- The dissociation energies of water and six models of aromatic compounds were computed at a B3LYP/6 level, with the bond dissociation energies of the five aromatic compounds found to be less than that of the corresponding HO—H dissociation energy of H_2O. This indicates that radical processes are likely to be responsible for the observed changes in aromatic content.

- Switching the initiator used in the ultrasonic reactions of creosote oil from Fe^{2+} to Ni^{2+} results in a change in product enrichment from acenaphthalene to naphthalene and phenanthrene.

■ AUTHOR INFORMATION

Corresponding Author

Yu-Fang Ye — *College of Chemistry and Chemical Engineering, Xinjiang Normal University, Urumqi 830054, China;* ⊙ orcid.org/0000-0003-2566-8165; Phone: +86 0991 4333139; Email: 34229636@qq.com

Authors

Ying Zhu — *College of Chemistry and Chemical Engineering, Xinjiang Normal University, Urumqi 830054, China*

Zhi Su — *College of Chemistry and Chemical Engineering, Xinjiang Normal University, Urumqi 830054, China*

Feng-Yun Ma — *College of Chemistry and Chemical Engineering, Xinjiang Normal University, Urumqi 830054, China*

Ting Liang — *College of Chemistry and Chemical Engineering, Xinjiang Normal University, Urumqi 830054, China*

Complete contact information is available at:
https://pubs.acs.org/10.1021/acsomega.0c06357

Notes

The authors declare no competing financial interest.

■ ACKNOWLEDGMENTS

■ REFERENCES

(1) Morgan, T. J.; George, A.; Álvarez, P.; Millan, M.; Herod, A. A.; Kandiyoti, R. Characterization of Molecular Mass Ranges of Two Coal Tar Distillate Fractions (Creosote and Anthracene Oils) and Aromatic Standards by LD-MS, GC-MS, Probe-MS and Size-exclusion Chromatography. *Energy Fuels* 2008, 22, 3275−3292.

(2) King, M. W. G.; Barker, J. F.; Devlin, J. F.; Butler, B. J. Migration and natural fate of a coal tar creosote plume 2. Mass balance and biodegradation indicators. *J. Contam. Hydrol.* 1999, 39, 281−307.

(3) Polcaro, C. M.; Brancaleoni, E.; Donati, E.; Frattoni, M.; Galli, E.; Migliore, L.; Rapana, P. Fungal Bioremediation of Creosote-Treated Wood: A Laboratory Scale Study on Creosote Components Degradation by Pleurotus ostreatus Mycelium. *Bull. Environ. Contam. Toxicol.* 2008, 81, 180−184.

(4) Ren, X. E.; Li, C. Z.; Yang, F.; Huang, Y. C.; Huang, C. D.; Zhang, K. M.; Yan, L. J. Comparison of hydrodynamic and ultrasonic cavitation effects on soy protein isolate functionality. *J. Food Eng.* 2020, 265, No. 109697.

(5) Thanekar, P.; Garg, S.; Gogate, P. R. Hybrid treatment strategies based on hydrodynamic cavitation, advanced oxidation processes, and aerobic oxidation for efficient removal of naproxen. *Ind. Eng. Chem. Res.* 2020, 59, 4058−4070.

(6) Yi, C. H.; Lu, Q. Q.; Wang, Y.; Wang, Y. X.; Yang, B. L. Degradation of organic wastewater by hydrodynamic cavitation combined with acoustic cavitation. *Ultrason. Sonochem.* 2018, 43, 156−165.

(7) Cai, M. Q.; Hu, J. Q.; Lian, G. H.; Xiao, R. Y.; Song, Z. J.; Jin, M. C.; Dong, C. Y.; Wang, Q. Y.; Luo, D. W.; Wei, Z. S. Synergetic pretreatment of waste activated sludge by hydrodynamic cavitation combined with Fenton reaction for enhanced dewatering. *Ultrason. Sonochem.* 2018, 42, 609−618.

(8) Boczkaj, G.; Gągol, M.; Klein, M.; Przyjazny, A. Effective method of treatment of effluents from production of bitumens under basic pH conditions using hydrodynamic cavitation aided by external oxidants. *Ultrason. Sonochem.* 2018, 40, 969−979.

(9) Ye, Y. F.; Ma, F. Y.; Wu, M.; Wei, X. Y.; Liu, J. M. Increase of acenaphthene content in creosote oil by hydrodynamic cavitation. *Chem. Eng. Process.* 2016, 104, 66−74.

(10) Gogate, P. R. Cavitational reactors for process intensification of chemical processing applications: A critical review. *Chem. Eng. Process.* 2008, 47, 515−527.

(11) Kalumuck, K.; Chahine, G. The use of cavitating jets to oxidize organic compounds in water. *J. Fluids Eng.* 2000, 122, 465−470.

(12) Cai, M. Q.; Su, J.; Zhu, Y. Z.; Wei, X. Q.; Jin, M. C.; Zhang, H. J.; Dong, C. Y.; Wei, Z. S. Decolorization of azo dyes Orange G using hydrodynamic cavitation coupled with heterogeneous Fenton process. *Ultrason. Sonochem.* 2016, 28, 302−310.

(13) Gogate, P. R.; Pandit, A. B. Hydrodynamic cavitation reactors: A State of the art review. *Rev. Chem. Eng.* 2001, 17, 1−85.

(14) Gogate, P. R.; Pandit, A. B. A review and assessment of hydrodynamic cavitation as a technology for the future. *Ultrason. Sonochem.* 2005, 12, 21−27.

(15) Hoffmann, M. R.; Hua, I.; Hochemer, R. Application of ultrasonic irradiation for degradation of chemical contaminants in water. *Ultrason. Sonochem.* 1996, 3, S163−S172.

(16) Pandit, A. B.; Moholkal, V. S. Harness cavitation to improve processing. *Chem. Eng. Prog.* 1996, 7, 57−69.

(17) Sivakumar, M.; Pandit, A. B. Wastewater treatment: a novel energy efficient hydrodynamic cavitational technique. *Ultrason. Sonochem.* 2002, 9, 123−131.

(18) Didenko, Y. T.; Suslick, K. S. The energy efficiency of formation of photons, radicals and ions during single-bubble cavitation. *Nature* 2002, 418, 394−397.

(19) Prajapat, A. L.; Gogate, P. R. Intensification of depolymerization of aqueous guar gum using hydrodynamic cavitation. *Chem. Eng. Process.* 2015, 93, 1−9.

(20) Patil, P. N.; Gogate, P. R. Degradation of methyl parathion using hydrodynamic cavitation: Effect of operating parameters and intensification using additives. *Sep. Purif. Technol.* 2012, 95, 172−179.

(21) Shriwas, A. K.; Gogate, P. R. Ultrasonic degradation of methyl Parathion in aqueous solutions: Intensification using additives and scale up aspects. *Sep. Purif. Technol.* 2011, 79, 1−7.

(22) Gogate, P. R.; Rajiv, K.; Pandit, A. B. Cavitation: A technology on the horizon. *Curr. Sci.* 2006, 91, 35−46.

(23) Joshi, R. K.; Gogate, P. R. Degradation of dichlorvos using hydrodynamic cavitation based treatment strategies. *Ultrason. Sonochem.* 2012, 19, 532−539.

(24) Badve, M.; Gogate, P.; Pandit, A.; Csoka, L. Hydrodynamic cavitation as a novel approach for wastewater treatment in wood finishing industry. *Sep. Purif. Technol.* 2013, 106, 15−21.

(25) Wu, Z.; Shen, H. F.; Ondruschka, B.; Zhang, Y.; Wang, W.; Bremne, D. H. Removal of blue-green algae using the hybrid method of hydrodynamic cavitation and ozonation. *J. Hazard. Mater.* 2012, 235−236, 152−158.

(26) Schwetlick, K. Organikum. Weinheim, Federal Republic of Germany, 2004, pp 129 130.